

# Generation and control of Doppler harmonics approaching $10^{22} \text{W/cm}^2$ on plasma mirrors

Baptiste Groussin,<sup>1</sup> Philipp Sikorski,<sup>2</sup> Aodhan McIlvenny,<sup>3</sup> Kosta Oubrerie,<sup>2</sup> Pierre Bartoli,<sup>2</sup> Lieselotte Obst-Huebl,<sup>3</sup> Anthony Vazquez,<sup>3,4</sup> Lulu Russell,<sup>3,4</sup> Tirtha Mandal,<sup>3,\*</sup> Kei Nakamura,<sup>3</sup> Anthony J. Gonsalves,<sup>3</sup> Cameron G. R. Geddes,<sup>3</sup> Luca Fedeli,<sup>2</sup> Henri Vincenti,<sup>2</sup> and Adrien Leblanc<sup>1</sup>

<sup>1</sup>*Laboratoire d'Optique Appliquée (LOA),*

*CNRS, École polytechnique, ENSTA,*

*Institut Polytechnique de Paris, Palaiseau, France*

<sup>2</sup>*Université Paris-Saclay, CEA, LIDYL, 91191 Gif-sur-Yvette, France*

<sup>3</sup>*Lawrence Berkeley National Laboratory,*

*1 Cyclotron Road, Berkeley, California, 94720, USA*

<sup>4</sup>*University of California, Berkeley, California, 94720, USA*

(Dated: February 12, 2026)

## Abstract

In this letter, we report Doppler harmonic generation with a relativistic plasma mirror at unprecedented intensities  $> 10^{21} \text{ W/cm}^2$  using a PetaWatt-class laser. We show that beyond a few  $10^{21} \text{ W/cm}^2$  a precise control of the laser contrast at the sub-picosecond time scale becomes essential to drive the efficient generation of high-order harmonics. Such control is paramount for deploying plasma mirrors in high-field applications at PetaWatt-class laser facilities, including, for instance, their use as intensity boosters in the pursuit of the strong-field regime of quantum electrodynamics.

PACS numbers: Valid PACS appear here

The advent of chirped-pulse amplification [1] has enabled light intensities high enough to drive matter into the relativistic regime, paving the way for the fields of relativistic optics [2] and ultra-high intensity science [3–6]. In this context, plasma mirrors [7, 8] have emerged as key optical elements for manipulating ultra-intense light [9–15]. They are formed when a tightly focused femtosecond laser pulse ionizes a solid target, producing a dense plasma that reflects the incident light. When the plasma–vacuum interface has a density gradient of scale length  $L$  much shorter than the laser wavelength  $\lambda$ , the plasma surface behaves as a mirror of excellent optical quality [16–18].

Plasma mirrors have proven essential for applications ranging from laser-driven ion acceleration [6, 19, 20] to high-order harmonic generation (HHG) [4, 21], the latter being central to the present work. Harmonics up to the extreme ultraviolet (XUV) spectral region can be generated via the Doppler effect by the relativistic oscillations of the surface of a plasma mirror irradiated at ultra-high intensities [4, 22–25]. Initially envisioned as a source to perform attosecond pump-probe experiments [26] and probe relativistic laser–plasma interactions [27], Doppler harmonic generation has recently attracted renewed interest as a promising route to boost PW-class laser intensities by several orders of magnitude [28–33]. Simulations predict that successfully operating plasma mirrors in the multi PW-regime could yield boosted laser intensities well above  $10^{25} \text{ W/cm}^2$ , opening a pathway [34–38] to probe the strong-field regime of quantum electrodynamics (QED)[5, 39]. This intensification arises from a relativistic spatiotemporal compression: as the laser drives the plasma mirror surface to oscillate at relativistic velocities, each optical cycle experiences temporal compression

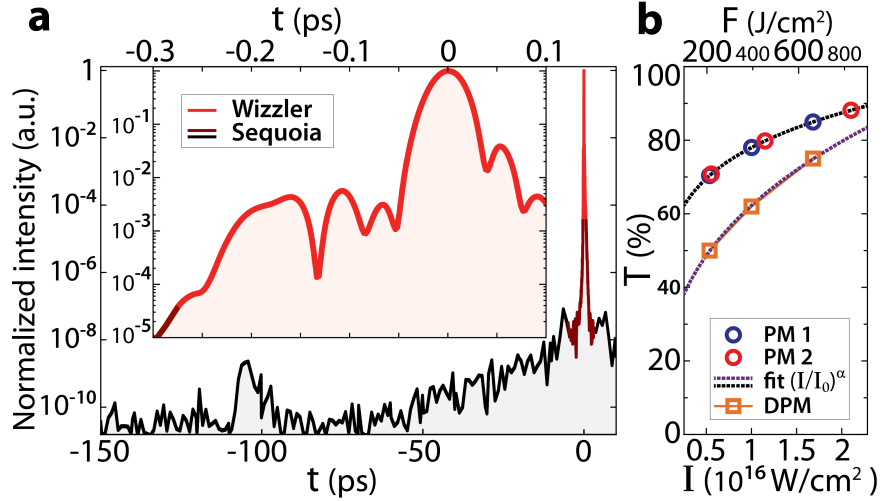


FIG. 1. (a) Laser temporal profile measured with a Sequoia cross-correlator: -150ps window / 0.9ps resolution in black,  $\pm 5\text{ps}$  window / 0.1ps resolution in red. Inset: sub-300fs Wizzler measurement before the DPM. (b) DPM transmission as a function of the maximum intensity and fluence incident on the first PM surface (orange markers). The deduced transmissions of each plasma mirror (red and blue circles) are shown as a function of the intensity on each PM surface (black and purple lines), obtained from a power-law fit (see Sup. Mat. [51])

and Doppler upshifting into the XUV, while the plasma curvature — induced by the laser radiation pressure — focuses the emitted radiation.

Enabling plasma mirrors in such applications requires preserving a sharp gradient scale length. This is a real challenge as it requires a high laser contrast, commonly defined as the ratio of the peak intensity to that of the nanosecond-scale pedestal preceding the main pulse. This pedestal can pre-ionize and heat the target, driving unwanted plasma expansion and degrading the interface unless properly suppressed [9, 18]. To this end, various contrast-enhancement techniques have been developed, the most common involving “optical switches” that transmit the pedestal but become ionized at a threshold intensity, acting as ultrafast shutters [7, 8, 40–42]. By achieving laser contrast better than  $10^{12}$  [43–48], these devices have proven highly effective to drive relativistic plasma mirrors in applications using high-power lasers [49] at intensities well below  $10^{21} \text{ W/cm}^2$ , with only one recent work [50] reaching  $1.2 \times 10^{21} \text{ W/cm}^2$ .

In this Letter, we report the first study of Doppler harmonic generation from plasma mirrors at intensities substantially exceeding  $10^{21} \text{ W/cm}^2$  and approaching  $10^{22} \text{ W/cm}^2$ , using a PW-class laser. By measuring XUV harmonic properties as a function of laser and plasma mirror parameters, we show that for peak intensities above few  $10^{21} \text{ W/cm}^2$  the laser

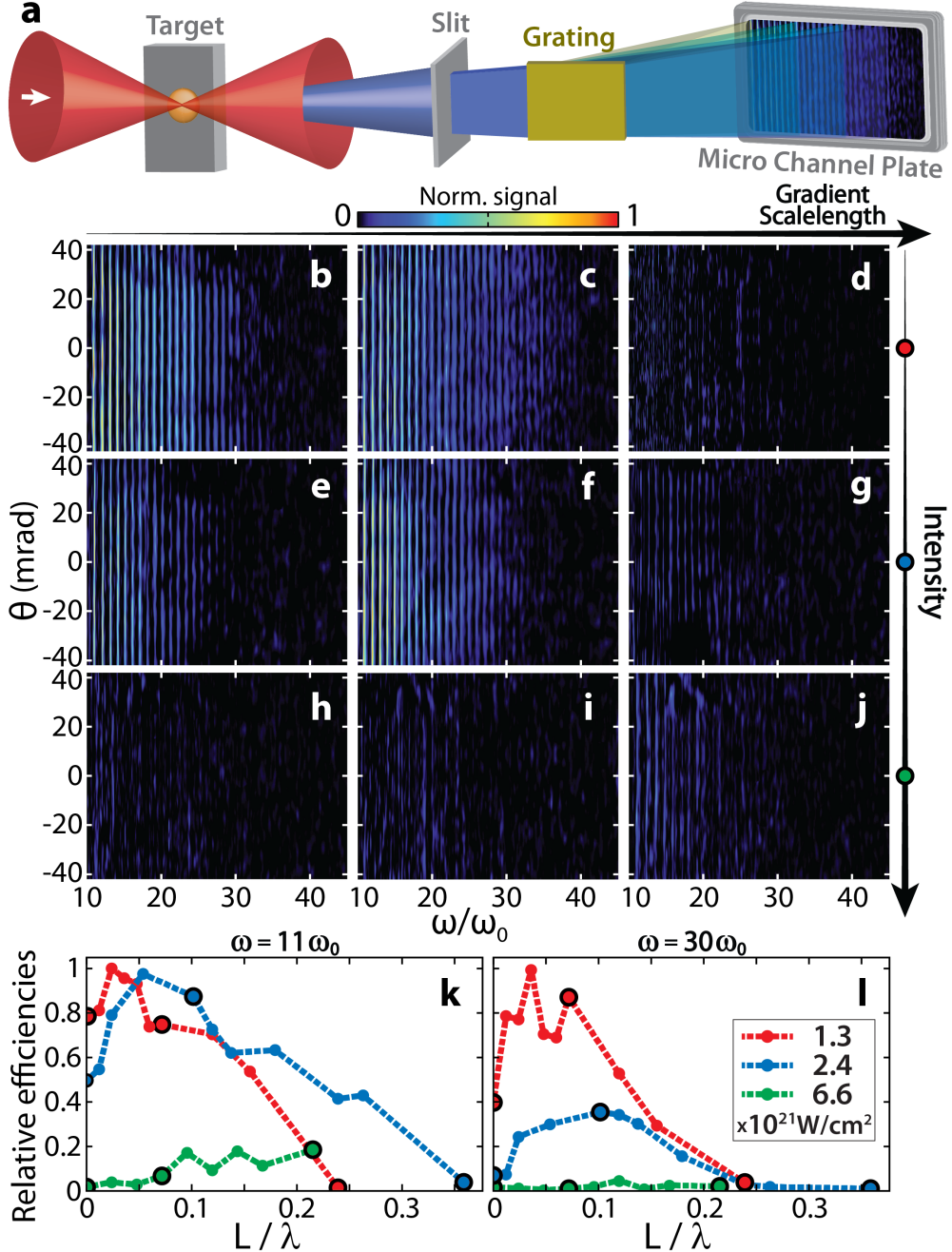


FIG. 2. (a) Experimental scheme: the laser is focused onto the pre-ionized target and the XUV spectrum is measured using a 2-mm entrance slit and a curved XUV grating imaging the HHG source (in the dispersive direction) onto a micro-channel-plate detector coupled to a phosphor screen imaged by a camera. (b-j) Angularly resolved XUV spectra for different on-target laser intensities:  $1.3 \times 10^{21} \text{ W/cm}^2$  (b-d),  $2.4 \times 10^{21} \text{ W/cm}^2$  (e-g), and  $6.6 \times 10^{21} \text{ W/cm}^2$  (h-j), and for different gradient scale lengths: short ( $L = 0$ , first column), intermediate ( $L \approx \lambda/11$ , second column), and long ( $L > \lambda/5$ , third column). All spectra are normalized to the maximum value across the entire dataset. (k-l) Relative efficiency of the 11<sup>th</sup> (k) and 30<sup>th</sup> (l) harmonics as a function of the plasma gradient length, calculated as the sum of the signal within a 6mrad  $\times$  85mrad angular window. For each harmonic order, the efficiencies are normalized to the maximum value across the entire dataset. Data points corresponding to panels (b-j) are marked with a black contour.

pedestal at the sub-picosecond (ps) time scale becomes a critical factor affecting plasma mirror quality and harmonic generation efficiency. Building on these results, we propose new contrast-enhancement strategies tailored for PW-class facilities, which will be crucial for operating plasma mirrors under optimal conditions in next-generation high-intensity applications.

The experiment was conducted at the BELLA PW laser facility [52] LBNL (US). Pulses with an energy up to 30.6 J after compression down to 37-fs Full Width Half Maximum (FWHM) duration were used. The pulse temporal profile is presented in Fig. 1(a). Temporal contrast enhancement was achieved using a double-plasma-mirror (DPM) system (see design in the Supplementary Material (Sup. Mat.) [51]). The total DPM transmission, along with the inferred transmission of each plasma mirror (see Sup. Mat. [51]) and the corresponding fluences/intensities on their surfaces, is presented in Fig. 1(b). These measurements show excellent agreement with previous reports [8, 46, 53–55] (see Sup. Mat. [51]).

After the DPM, the beam is focused down to a  $2.8\text{ }\mu\text{m}$  FWHM focal spot onto a  $\text{SiO}_2$  polished target, using a 0.5 m off-axis parabola in the BELLA iP2 target chamber. A 9 mm pick-off mirror positioned upstream from the final parabola samples a small portion of the beam, which is loosely focused to a  $48\text{ }\mu\text{m}$  FWHM spot at a few  $10^{15}\text{ W/cm}^2$ , with an adjustable delay relative to the main pulse for pre-ionizing the target and controlling the gradient scalelength during the interaction to optimize HHG yield [17]. The plasma expansion velocity was measured [56] with equivalent fluences on target at LOA with the Salle Jaune laser to lie between 15 and 30 nm/ps in good agreement with prior studies [17, 18].

As illustrated in Fig. 2(a), an XUV spectrometer was placed in the specular direction of the reflected beam to record the angular profile of harmonics above the 11<sup>th</sup> order with an angular acceptance of 6 mrad (slit width) by 85 mrad (limited by the grating width). Consequently, only a fraction of the XUV beam could be measured.

XUV spectra were recorded for several gradient scale lengths for three laser energies: 9.8 J, 18.2 J, and 30.6 J on DPM, corresponding to 4.9 J, 11.3 J, and 22.9 J on target and intensities of 1.3, 2.4, and  $6.6 \times 10^{21}\text{ W/cm}^2$ , respectively. For each intensity, three representative angularly resolved spectra are shown in Figs. 2 (b–j), corresponding to short ( $L = 0$ ), intermediate ( $L \approx \lambda/11$ ), and long ( $L > \lambda/5$ ) gradients. The XUV signals integrated over the spectrometer angular window are plotted as a function of the gradient scale length for

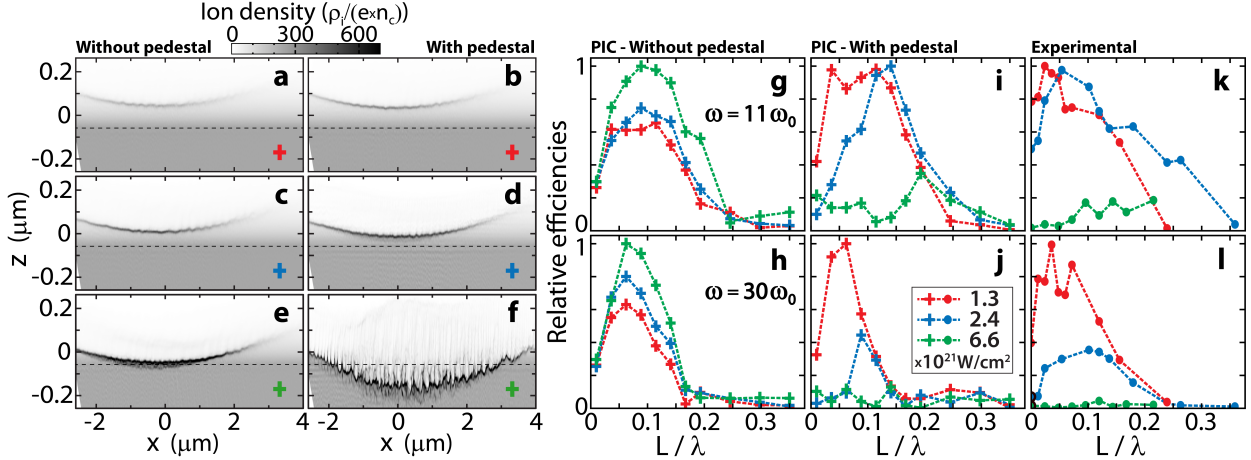


FIG. 3. High-resolution PIC simulations corresponding to the experimental cases. (a–f) For an initial plasma gradient length of  $\lambda/10$ : target ion density at the peak of the laser pulse for intensities of  $1.3 \times 10^{21} \text{ W/cm}^2$  (a–b),  $2.4 \times 10^{21} \text{ W/cm}^2$  (c–d), and  $6.6 \times 10^{21} \text{ W/cm}^2$  (e–f). First column (a,c,e): idealized 37 fs FWHM Gaussian laser pulse (no pedestal); second column (b,d,f): realistic laser temporal profile (with pedestal). In each panel, the black dashed line delimits the initial boundary between the plasma gradient and the bulk region. (g–l) Harmonic generation efficiency for the 11<sup>th</sup> (first row) and 30<sup>th</sup> (second row) orders as a function of plasma scale length, calculated as the sum of the harmonic signal collected by the detector (or within the same 85 mrad angular window for numerical data), for the three intensities on target: 1.3 (red lines), 2.4 (blue), and  $6.6 \times 10^{21} \text{ W/cm}^2$  (green). Harmonic efficiency from PIC simulations without pedestal, first column (g–h), with realistic laser temporal profile, second column (i–j), compared with the experimental harmonic efficiencies from Fig. 2, last column (k–l). For each panel, the efficiencies are normalized with respect to the maximum value.

harmonic orders 11<sup>th</sup> and 30<sup>th</sup> in Figs. 2(k) and (l). These results reveal a strong decrease of the harmonic emission efficiency with increasing laser intensity: high-order harmonics up to the 40<sup>th</sup> and 30<sup>th</sup> orders are observed at optimized gradients for 1.3 and  $2.4 \times 10^{21} \text{ W/cm}^2$ , respectively, but a very low harmonic signal is detected at  $6.6 \times 10^{21} \text{ W/cm}^2$ .

In order to gain insights on how HHG is affected by the interplay of the laser temporal contrast and of the plasma gradient scale length, we carried out an extensive numerical simulation campaign, using the high-performance Particle-In-Cell [57, 58] (PIC) code WarpX v 25.09 [59, 60]. Simulations were carried out in 2D geometry to allow exploring a large parameter space (see Sup. Mat. [51] for a detailed description of the numerical setup, and also references [61–64] therein).

By comparing the experimental results with kinetic plasma simulations, we show that the reduction in XUV emission efficiency with the laser intensity originates from the sub-ps pedestal preceding the main pulse. As shown in Fig. 1(a), the temporal profile exhibits a

sub-300-fs pedestal with a contrast of a few  $10^{-3}$ , typical of lasers in this class [44, 55] and inevitably arising from fine spectral modulations. With an average contrast of  $2.7 \times 10^{-3}$  in the -220 to -50 fs temporal window, such pedestal reaches relativistic intensities several hundreds of fs prior to the main pulse, potentially leading to a significant degradation of the plasma-mirror surface quality, as shown in Figs. 3(a–f).

Plasma mirrors typically ionize at intensities on the order of few  $10^{13}$  W/cm<sup>2</sup> [7, 8, 40, 45]. Assuming a DPM ionization triggering intensity of  $2 \times 10^{13}$  W/cm<sup>2</sup>, the temporal profiles of the laser reflected from the DPM can be inferred (see Sup. Mat. [51]). For the three experimental cases with energies after compression of 9.8, 18.2, and 30.6 J, this analysis yields sub-ps contrasts with average values of  $2.8 \times 10^{-5}$ ,  $1.1 \times 10^{-3}$ , and  $1.8 \times 10^{-3}$  during temporal windows of 110 fs, 175 fs, and 200 fs prior to the pulse peak power, respectively. These contrast levels correspond to target illumination before the arrival of the main pulse at intensities of  $3.6 \times 10^{16}$  W/cm<sup>2</sup> over 110 fs,  $2.6 \times 10^{18}$  W/cm<sup>2</sup> over 175 fs, and  $1.1 \times 10^{19}$  W/cm<sup>2</sup> over 200 fs, respectively. PIC simulations clearly indicate that such pedestals are sufficient to heat the target plasma-mirror surface and degrade its quality, see Figs. 3 (a-f).

In the absence of a pedestal, simulations show that the harmonic yield increases with the intensity on target, and that the harmonic efficiency is maximized for a plasma density gradient scale length of  $L \sim \lambda/10$ , independently of the peak laser intensity, see Figs. 3(g–h), which is in agreement with previous numerical studies [30]. When the pedestal is included, the simulations indicate that the harmonic yield drops significantly with increasing intensity, leading to a collapse of harmonic generation at  $6.6 \times 10^{21}$  W/cm<sup>2</sup>. In addition, Figs. 3 (i–j) show that the optimal scale length shifts toward larger values as the peak intensity increases. These results are in very good agreement with the experimental observations, Figs. 2(k–l) (reproduced in Figs. 3(k-l)). The efficiency drop may be attributed to the radiation pressure exerted by the pedestal, which dents the plasma and induces a surface density modulation, as clearly visible in Fig. 3(f). This modulations is reminiscent of those attributed to filamentation instability in laser-solid interaction[65, 66], albeit in different regimes. Previous studies have shown that HHG is severely affected by surface corrugations when the root-mean-square roughness is greater than  $\approx 100$  nm [11], which is approximately the amplitude of the surface modulation in Fig. 3(f). Moreover, laser interaction with modulated surfaces is associated with a more efficient energy absorption[67], which in our case may accelerate the disruption of the target surface. Finally, we observe that the radiation

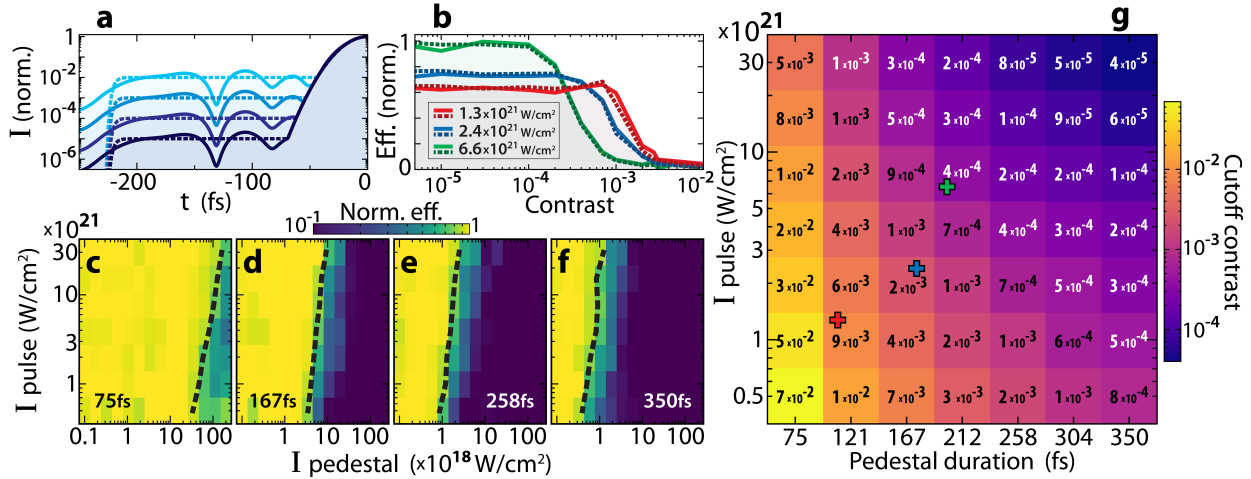


FIG. 4. PIC simulations to investigate the impact of sub-ps contrast on HHG efficiency of the 11<sup>th</sup> order for a plasma scale length of  $\lambda/10$  (optimizing HHG in the absence of pedestal, see Fig.3(g)). For a more general study of HHG efficiency, no angular filtering corresponding to a specific detector window is applied here. (a,b) HHG efficiency, panel (b), for the three experimental main pulse intensities as a function of the average sub-220 fs temporal contrast, panel (a), using a realistic temporal profile (the one of the laser before the DPM), solid lines, and a simplified 220 fs super-Gaussian profile (order 60), dashed lines. (c–f) HHG efficiency versus sub-350fs pedestal intensity and main pulse intensity for a super-Gaussian pedestal whose duration is 75 fs (c), 167 fs (d), 258 fs (e), and 350 fs (f). Black dashed lines indicate the pedestal intensity cutoff, defined as where the HHG efficiency drops below 70% of the pedestal-free case. (g) Deduced cutoff contrasts for controlled laser–plasma interaction as a function of pedestal duration and on-target main pulse intensity. Colored crosses mark the three probed experimental conditions.

pressure shortens the controlled density gradient formed by the pre-pulse (see Fig. 3(a-f)), possibly shifting the interaction conditions from those required for optimal HHG. While it is plausible that the collapse of HHG efficiency that we have observed may be attributed to a combination of these effects, a detailed investigation is beyond the scope of the present manuscript, and will be the object of a dedicated study.

Higher harmonic orders with shorter wavelengths are more sensitive to this spatial modulation, and their efficiency decreases more rapidly with increasing laser intensity. In addition, the radiation pressure shortens the controlled density gradient formed by the pre-pulse, which could explain why longer initial scale lengths are required to optimize the HHG efficiency.

In the light of these observations, we now use PIC simulations to assess the threshold laser contrast required for efficient HHG as a function of the peak laser intensity on target and the sub-ps pedestal duration, see Fig. 4. For more general conclusions, panels (a–b) show

that realistic and simplified super-Gaussian pedestals with the same average contrast have equivalent effects, so the systematic study of pulse intensity, pedestal duration, and contrast is carried out using only considering a super-Gaussian pedestal. As the peak intensity increases, a higher temporal contrast is required for a given pedestal duration, Fig. 4(b). Similarly, for longer pedestal durations, the required contrast rises rapidly, Figs. 4(c–f). The laser contrast threshold as a function of both pedestal duration and peak intensity is summarized in Fig. 4(g), providing an important roadmap for optimizing HHG with plasma mirrors at extreme intensities.

This roadmap notably indicates that DPM systems currently available at PW-class facilities, primarily designed to improve the nanosecond temporal contrast, are not yet suited for a precise control of laser–plasma interaction at intensities beyond  $\sim 10^{21} \text{ W/cm}^2$ . In this regard, our work provides essential guidelines for the tuning of DPM systems to enhance laser contrast at such extreme intensities. A simple design solution for a DPM is to position the first plasma mirror (PM1) so that the short-delay pedestal fluence remains below  $\sim 1 - 2 \times 10^{13} \text{ W/cm}^2$  at its surface. For instance, cleaning a sub-ps contrast of  $3 \times 10^{-3}$  would require limiting the maximum peak intensity onto PM1 below  $\sim 3 - 5 \times 10^{15} \text{ W/cm}^2$ , at the expense of reducing the transmitted energy. This energy loss can be compensated by operating the second plasma mirror (PM2) at a higher fluence ( $> 2 \times 10^{16} \text{ W/cm}^2$ ) to maximize its reflectivity. For the BELLA facility, this would require setting PM1  $\sim 30 \text{ cm}$  (instead of 17.5 cm) before the focus of the 13.5 m parabola and would result in reflectivities of  $\sim 70\%$  and  $\sim 88\%$  on PM1 and PM2 respectively, see Fig. 1(b), corresponding to a total DPM transmittance of  $\sim 62\%$ , a modest drop with respect to the  $\sim 75\%$  transmittance of the present configuration at maximum power.

As a summary, we report the first demonstration of Doppler harmonic generation on plasma mirrors at record peak intensities above  $10^{21} \text{ W/cm}^2$ . By operating at this extreme, we uncover a previously unrecognized boundary for further scaling : beyond this intensity, the harmonic yield drops abruptly as the sub-picosecond pedestal becomes a dominant factor governing interaction control. This limitation had not been identified previously, either theoretically—where idealized laser pulses are typically assumed—or experimentally, since on-target intensities have so far been limited to  $\sim 10^{21} \text{ W/cm}^2$  [50]. Importantly, we propose a clear path forward for operating contrast-enhancement systems at PW-class facilities and enable efficient plasma-mirror control beyond  $10^{21} \text{ W/cm}^2$ , paving the way for

ultra-high-intensity applications, including access to the strong-field QED regime.

We gratefully acknowledge the support of Zachary Eisentraut, Mark Kirkpatrick, Federico Mazzini, Mackinley Kath, Joe Riley, Arturo Magana, Teo Maldonado Mancuso, Chetanya Jain, Nathan Ybarrolaza, Carl Schroeder, Jeroen van Tilborg, Jens Osterhoff, Derrick McGrew, Hai-En Tsai and Eric Esarey.

The work was supported by the U.S. Department of Energy's (DOE) Office of Science (SC) Fusion Energy Sciences (FES) program: the LaserNetUS initiative at the BELLA Center, and the Office of High Energy Physics (HEP), both under Contract No. DE-AC02-05CH11231

This project has received funding from the European Research Council (ERC) under the European Union's Horizon 2020 research and innovation program (grant agreement No. 101076814).

This research used the open-source particle-in-cell code WarpX. Primary WarpX contributors are with LBNL, LLNL, CEA-LIDYL, SLAC, DESY, CERN, Helion Energy, and TAE Technologies. We acknowledge all WarpX contributors.

This project was provided with computing HPC and storage resources by GENCI at CINES thanks to grants 2025-A0190516880, 2025-AD010515627R1, 2024-AD010515627, and 2024-A0140513434 on the supercomputer Adastra's MI250x partition.

We acknowledge the financial support of the Cross-Disciplinary Program on Instrumentation and Detection of CEA, the French Alternative Energies and Atomic Energy Commission.

This project has received funding from the European Union's Horizon Europe research and innovation programme under the Marie Skłodowska-Curie Doctoral Networks grant agreement No 101169117.

---

\* Current address: Raja Ramanna Centre for Advanced Technology, Indore 452013, India

- [1] D. Strickland and G. Mourou, Compression of amplified chirped optical pulses, *Optics Communications* **56**, 219 (1985).
- [2] G. A. Mourou, T. Tajima, and S. V. Bulanov, Optics in the relativistic regime, *Reviews of modern physics* **78**, 309 (2006).
- [3] E. Esarey, C. B. Schroeder, and W. P. Leemans, Physics of laser-driven plasma-based electron

accelerators, *Rev. Mod. Phys.* **81**, 1229 (2009).

[4] U. Teubner and P. Gibbon, High-order harmonics from laser-irradiated plasma surfaces, *Reviews of Modern Physics* **81**, 445 (2009).

[5] A. Di Piazza, C. Müller, K. Z. Hatsagortsyan, and C. H. Keitel, Extremely high-intensity laser interactions with fundamental quantum systems, *Rev. Mod. Phys.* **84**, 1177 (2012).

[6] A. Macchi, M. Borghesi, and M. Passoni, Ion acceleration by superintense laser-plasma interaction, *Rev. Mod. Phys.* **85**, 751 (2013).

[7] H. C. Kapteyn, M. M. Murnane, A. Szoke, and R. W. Falcone, Prepulse energy suppression for high-energy ultrashort pulses using self-induced plasma shuttering, *Opt. Lett.* **16**, 490 (1991).

[8] G. Doumy, F. Quéré, O. Gobert, M. Perdrix, P. Martin, P. Audebert, J. C. Gauthier, J.-P. Geindre, and T. Wittmann, Complete characterization of a plasma mirror for the production of high-contrast ultraintense laser pulses, *Phys. Rev. E* **69**, 026402 (2004).

[9] C. Thaury, F. Quere, J.-P. Geindre, A. Levy, T. Ceccotti, P. Monot, M. Bougeard, F. Réau, P. d’Oliveira, P. Audebert, *et al.*, Plasma mirrors for ultrahigh-intensity optics, *Nature Physics* **3**, 424 (2007).

[10] B. Dromey, S. Kar, C. Bellei, D. C. Carroll, R. J. Clarke, J. S. Green, S. Kneip, K. Markey, S. R. Nagel, P. T. Simpson, L. Willingale, P. McKenna, D. Neely, Z. Najmudin, K. Krushelnick, P. A. Norreys, and M. Zepf, Bright multi-kev harmonic generation from relativistically oscillating plasma surfaces, *Phys. Rev. Lett.* **99**, 085001 (2007).

[11] B. Dromey, D. Adams, R. Hörlein, Y. Nomura, S. Rykovanov, D. Carroll, P. Foster, S. Kar, K. Markey, P. McKenna, *et al.*, Diffraction-limited performance and focusing of high harmonics from relativistic plasmas, *Nature Physics* **5**, 146 (2009).

[12] M. Nakatsutsumi, A. Kon, S. Buffe, P. Audebert, J. Fuchs, and R. Kodama, Fast focusing of short-pulse lasers by innovative plasma optics toward extreme intensity, *Opt. Lett.* **35**, 2314 (2010).

[13] H. Vincenti, S. Monchocé, S. Kahaly, G. Bonnaud, P. Martin, and F. Quéré, Optical properties of relativistic plasma mirrors, *Nature communications* **5**, 3403 (2014).

[14] A. Denoeud, L. Chopineau, A. Leblanc, and F. Quéré, Interaction of ultraintense laser vortices with plasma mirrors, *Physical review letters* **118**, 033902 (2017).

[15] A. Leblanc, A. Denoeud, L. Chopineau, G. Mennerat, P. Martin, and F. Quéré, Plasma holograms for ultrahigh-intensity optics, *Nature Physics* **13**, 440 (2017).

[16] G. G. Scott, V. Bagnoud, C. Brabetz, R. J. Clarke, J. S. Green, R. I. Heathcote, H. W. Powell, B. Zielbauer, T. D. Arber, P. McKenna, and D. Neely, Optimization of plasma mirror reflectivity and optical quality using double laser pulses, *New Journal of Physics* **17**, 033027 (2015).

[17] S. Kahaly, S. Monchocé, H. Vincenti, T. Dzelzainis, B. Dromey, M. Zepf, P. Martin, and F. Quéré, Direct observation of density-gradient effects in harmonic generation from plasma mirrors, *Phys. Rev. Lett.* **110**, 175001 (2013).

[18] L. Chopineau, A. Leblanc, G. Blaclar, A. Denoeud, M. Thévenet, J.-L. Vay, G. Bonnaud, P. Martin, H. Vincenti, and F. Quéré, Identification of coupling mechanisms between ultraintense laser light and dense plasmas, *Physical Review X* **9**, 011050 (2019).

[19] D. Neely, P. Foster, A. Robinson, F. Lindau, O. Lundh, A. Persson, C.-G. Wahlström, and P. McKenna, Enhanced proton beams from ultrathin targets driven by high contrast laser pulses, *Applied Physics Letters* **89**, 021502 (2006).

[20] T. Ceccotti, A. Lévy, H. Popescu, F. Réau, P. D’Oliveira, P. Monot, J. P. Geindre, E. Lefebvre, and P. Martin, Proton acceleration with high-intensity ultrahigh-contrast laser pulses, *Phys. Rev. Lett.* **99**, 185002 (2007).

[21] J. Gao, F. Liu, X. Ge, Y. Deng, G. Zhang, Y. Fang, W. Wei, S. Yang, X. Yuan, M. Chen, Z. Sheng, and J. Zhang, Influence of laser contrast on high-order harmonic generation from solid-density plasma surfaces, *Chin. Opt. Lett.* **15**, 081902 (2017).

[22] S. V. Bulanov, N. M. Naumova, and F. Pegoraro, Interaction of an ultrashort, relativistically strong laser pulse with an overdense plasma, *Physics of Plasmas* **1**, 745 (1994).

[23] R. Lichters, J. Meyer-ter-Vehn, and A. Pukhov, Short-pulse laser harmonics from oscillating plasma surfaces driven at relativistic intensity, *Physics of Plasmas* **3**, 3425 (1996).

[24] C. Thaury and F. Quéré, High-order harmonic and attosecond pulse generation on plasma mirrors: basic mechanisms, *Journal of Physics B: Atomic, Molecular and Optical Physics* **43**, 213001 (2010).

[25] H. Yun, L. J. Bae, M. Mirzaie, and H. T. Kim, Laser-plasma-based radiation sources with intense laser pulses, *Reviews of Modern Plasma Physics* **9**, 13 (2025).

[26] Y. Nomura, R. Hörlein, P. Tzallas, B. Dromey, S. Rykovanov, Z. Major, J. Osterhoff, S. Karsch, L. Veisz, M. Zepf, *et al.*, Attosecond phase locking of harmonics emitted from laser-produced plasmas, *Nature Physics* **5**, 124 (2009).

[27] K. Krushelnick, I. Watts, M. Tatarakis, A. Gopal, U. Wagner, F. N. Beg, E. L. Clark, R. J. Clarke, A. E. Dangor, P. A. Norreys, M. S. Wei, and M. Zepf, Using self-generated harmonics as a diagnostic of high intensity laser-produced plasmas, *Plasma Physics and Controlled Fusion* **44**, B233 (2002).

[28] S. Gordienko, A. Pukhov, O. Shorokhov, and T. Baeva, Coherent focusing of high harmonics: A new way towards the extreme intensities, *Phys. Rev. Lett.* **94**, 103903 (2005).

[29] A. A. Gonoskov, A. V. Korzhimanov, A. V. Kim, M. Marklund, and A. M. Sergeev, Ultra-relativistic nanoplasmatics as a route towards extreme-intensity attosecond pulses, *Physical Review E—Statistical, Nonlinear, and Soft Matter Physics* **84**, 046403 (2011).

[30] H. Vincenti, Achieving extreme light intensities using optically curved relativistic plasma mirrors, *Phys. Rev. Lett.* **123**, 105001 (2019).

[31] F. Quéré and H. Vincenti, Reflecting petawatt lasers off relativistic plasma mirrors: a realistic path to the schwinger limit, *High Power Laser Science and Engineering* **9**, e6 (2021).

[32] L. Chopineau, A. Denoeud, A. Leblanc, E. Porat, P. Martin, H. Vincenti, and F. Quéré, Spatio-temporal characterization of attosecond pulses from plasma mirrors, *Nature physics* **17**, 968 (2021).

[33] H. Vincenti, T. Clark, L. Fedeli, P. Martin, A. Sainte-Marie, and N. Zaim, Plasma mirrors as a path to the schwinger limit: theoretical and numerical developments, *The European Physical Journal. ST, Special Topics* **232**, 2303 (2023).

[34] F. Karbstein, A. Blinne, H. Gies, and M. Zepf, Boosting quantum vacuum signatures by coherent harmonic focusing, *Phys. Rev. Lett.* **123**, 091802 (2019).

[35] L. Fedeli, A. Sainte-Marie, N. Zaim, M. Thévenet, J. L. Vay, A. Myers, F. Quéré, and H. Vincenti, Probing strong-field qed with doppler-boosted petawatt-class lasers, *Phys. Rev. Lett.* **127**, 114801 (2021).

[36] A. Sainte-Marie, L. Fedeli, N. Zaïm, F. Karbstein, and H. Vincenti, Quantum vacuum processes in the extremely intense light of relativistic plasma mirror sources, *New Journal of Physics* **24**, 065005 (2022).

[37] D.-X. Hui, Z.-H. Hu, X.-X. Mei, and Y.-N. Wang, Optimization of e+/e- pair yield during the interaction of a doppler-boosted laser with a solid-density plasma, *AIP Advances* **13**, 075214 (2023).

[38] N. Zaïm, A. Sainte-Marie, L. Fedeli, P. Bartoli, A. Huebl, A. Leblanc, J.-L. Vay, and H. Vin-

centi, Light-matter interaction near the schwinger limit using tightly focused doppler-boosted lasers, *Phys. Rev. Lett.* **132**, 175002 (2024).

[39] A. Gonoskov, T. G. Blackburn, M. Marklund, and S. S. Bulanov, Charged particle motion and radiation in strong electromagnetic fields, *Rev. Mod. Phys.* **94**, 045001 (2022).

[40] B. Dromey, S. Kar, M. Zepf, and P. Foster, The plasma mirror—a subpicosecond optical switch for ultrahigh power lasers, *Review of Scientific Instruments* **75**, 645 (2004).

[41] Y. Nomura, L. Veisz, K. Schmid, T. Wittmann, J. Wild, and F. Krausz, Time-resolved reflectivity measurements on a plasma mirror with few-cycle laser pulses, *New Journal of Physics* **9**, 9 (2007).

[42] R. Hörlein, B. Dromey, D. Adams, Y. Nomura, S. Kar, K. Markey, P. Foster, D. Neely, F. Krausz, G. D. Tsakiris, and M. Zepf, High contrast plasma mirror: spatial filtering and second harmonic generation at  $10^{19} \text{ wcm}^{-2}$ , *New Journal of Physics* **10**, 083002 (2008).

[43] K. Nakamura, H.-S. Mao, A. J. Gonsalves, H. Vincenti, D. E. Mittelberger, J. Daniels, A. Mangan, C. Toth, and W. P. Leemans, Diagnostics, control and performance parameters for the bella high repetition rate petawatt class laser, *IEEE Journal of Quantum Electronics* **53**, 1 (2017).

[44] H. Kiriyama, A. S. Pirozhkov, M. Nishiuchi, Y. Fukuda, K. Ogura, A. Sagisaka, Y. Miyasaka, M. Mori, H. Sakaki, N. P. Dover, K. Kondo, J. K. Koga, T. Z. Esirkepov, M. Kando, and K. Kondo, High-contrast high-intensity repetitive petawatt laser, *Opt. Lett.* **43**, 2595 (2018).

[45] L. Obst, J. Metzkes-Ng, S. Bock, G. E. Cochran, T. E. Cowan, T. Oksenhendler, P. L. Poole, I. Prencipe, M. Rehwald, C. Rödel, H.-P. Schlenvoigt, U. Schramm, D. W. Schumacher, T. Ziegler, and K. Zeil, On-shot characterization of single plasma mirror temporal contrast improvement, *Plasma Physics and Controlled Fusion* **60**, 054007 (2018).

[46] I. W. Choi, C. Jeon, S. G. Lee, S. Y. Kim, T. Y. Kim, I. J. Kim, H. W. Lee, J. W. Yoon, J. H. Sung, S. K. Lee, and C. H. Nam, Highly efficient double plasma mirror producing ultrahigh-contrast multi-petawatt laser pulses, *Opt. Lett.* **45**, 6342 (2020).

[47] L. Ranc, C. L. Blanc, N. Lebas, L. Martin, J.-P. Zou, F. Mathieu, C. Radier, S. Ricaud, F. Druon, and D. Papadopoulos, Improvement in the temporal contrast in the tens of ps range of the multi-pw apollon laser front-end, *Opt. Lett.* **45**, 4599 (2020).

[48] A. Kon, M. Nishiuchi, Y. Fukuda, K. Kondo, K. Ogura, A. Sagisaka, Y. Miyasaka, N. P. Dover, M. Kando, A. S. Pirozhkov, and et al., Characterization of the plasma mirror system

at the j-karen-p facility, High Power Laser Science and Engineering **10**, e25 (2022).

[49] C. N. Danson, C. Haefner, J. Bromage, T. Butcher, J.-C. F. Chanteloup, E. A. Chowdhury, A. Galvanauskas, L. A. Gizzi, J. Hein, D. I. Hillier, and et al., Petawatt and exawatt class lasers worldwide, High Power Laser Science and Engineering **7**, e54 (2019).

[50] R. Timmis, C. Fitzpatrick, J. Kennedy, H. Huddleston, E. Denis, A. James, C. Baird, D. Symes, D. McGonegle, E. Atonga, *et al.*, Relativistic harmonics in the efficiency limit, PREPRINT (Version 1) available at Research Square 10.21203/rs.3.rs-7284658/v1 (2025).

[51] See Supplemental Material at [URL] for a description of the experimental and numerical setups.

[52] K. Nakamura, H.-S. Mao, A. J. Gonsalves, H. Vincenti, D. E. Mittelberger, J. Daniels, A. Mangan, C. Toth, and W. P. Leemans, Diagnostics, control and performance parameters for the bella high repetition rate petawatt class laser, IEEE Journal of Quantum Electronics **53**, 1 (2017).

[53] S. Inoue, K. Maeda, S. Tokita, K. Mori, K. Teramoto, M. Hashida, and S. Sakabe, Single plasma mirror providing  $10^4$  contrast enhancement and 70% reflectivity for intense femtosecond lasers, Appl. Opt. **55**, 5647 (2016).

[54] T. Ziegler, D. Albach, C. Bernert, S. Bock, F.-E. Brack, T. E. Cowan, N. P. Dover, M. Garten, L. Gaus, R. Gebhardt, *et al.*, Proton beam quality enhancement by spectral phase control of a pw-class laser system, Scientific reports **11**, 7338 (2021).

[55] A. Kon, M. Nishiuchi, Y. Fukuda, K. Kondo, K. Ogura, A. Sagisaka, Y. Miyasaka, N. P. Dover, M. Kando, A. S. Pirozhkov, and et al., Characterization of the plasma mirror system at the j-karen-p facility, High Power Laser Science and Engineering **10**, e25 (2022).

[56] M. Bocoum, F. Böhle, A. Vernier, A. Jullien, J. Faure, and R. Lopez-Martens, Spatial-domain interferometer for measuring plasma mirror expansion, Optics Letters **40**, 3009 (2015).

[57] C. K. Birdsall and A. B. Langdon, *Plasma physics via computer simulation* (CRC press, 2018).

[58] T. D. Arber, K. Bennett, C. S. Brady, A. Lawrence-Douglas, M. G. Ramsay, N. J. Sircombe, P. Gillies, R. G. Evans, H. Schmitz, A. R. Bell, and C. P. Ridgers, Contemporary particle-in-cell approach to laser-plasma modelling, Plasma Physics and Controlled Fusion **57**, 113001 (2015).

[59] L. Fedeli, A. Huebl, F. Boillod-Cerneux, T. Clark, K. Gott, C. Hillairet, S. Jaure, A. Leblanc, R. Lehe, A. Myers, C. Piechurski, M. Sato, N. Zaim, W. Zhang, J.-L. Vay, and H. Vincenti,

Pushing the frontier in the design of laser-based electron accelerators with groundbreaking mesh-refined particle-in-cell simulations on exascale-class supercomputers, in *SC22: International Conference for High Performance Computing, Networking, Storage and Analysis* (2022) pp. 1–12.

- [60] J.-L. Vay, M. Acciarri, A. Almgren, L. D. Amorim, I. Andriyash, J. R. Angus, T. Antoun, D. Belkin, D. Bizzozero, A. Blelly, S. E. Clark, E. Dammak, L. Fedeli, A. Formenti, M. Garten, L. Ge, L. Giacomet, K. Gott, L. Giacomet, R. E. Groenewald, D. Grote, J. Gu, C. Harrison, M. Haseeb, A. Huebl, R. Jambunathan, I. Kara-Mostefa, H. Klion, P. Kumar, R. Lehe, B. Loring, T. Marks, P. Miller, A. Myers, J. Pech, E. Rheaume, G. Richardson, E. Rheaume, M. E. Rowan, R. T. Sandberg, P. Scherpelz, A. Sinn, O. Shapoval, D. Terzani, M. Thévenet, K. Weichman, E. Yang, N. Zaim, W. Zhang, Y. Zhao, K. Z. Zhu, and E. Zoni, WarpX: An advanced Particle-In-Cell code, <https://blast-warpX.github.io> (2025), <https://doi.org/10.5281/zenodo.17261711>.
- [61] J.-L. Vay, I. Haber, and B. B. Godfrey, A domain decomposition method for pseudo-spectral electromagnetic simulations of plasmas, *Journal of Computational Physics* **243**, 260 (2013).
- [62] H. Vincenti and J.-L. Vay, Detailed analysis of the effects of stencil spatial variations with arbitrary high-order finite-difference maxwell solver, *Computer Physics Communications* **200**, 147 (2016).
- [63] G. Blaclar, H. Vincenti, R. Lehe, and J. L. Vay, Pseudospectral maxwell solvers for an accurate modeling of doppler harmonic generation on plasma mirrors with particle-in-cell codes, *Phys. Rev. E* **96**, 033305 (2017).
- [64] M. Thévenet, I. A. Andriyash, L. Fedeli, Á. F. Pousa, A. Huebl, S. Jalas, M. Kirchen, R. Lehe, R. J. Shalloo, A. Sinn, *et al.*, Lasy: Laser manipulations made easy, arXiv preprint arXiv:2403.12191 (2024).
- [65] K. Quinn, L. Romagnani, B. Ramakrishna, G. Sarri, M. E. Dieckmann, P. A. Wilson, J. Fuchs, L. Lancia, A. Pipahl, T. Toncian, O. Willi, R. J. Clarke, M. Notley, A. Macchi, and M. Borghesi, Weibel-induced filamentation during an ultrafast laser-driven plasma expansion, *Phys. Rev. Lett.* **108**, 135001 (2012).
- [66] C. Schoenwaelder, A. Marret, S. Assenbaum, C. B. Curry, E. Cunningham, G. Dyer, S. Funk, G. D. Glenn, S. Goede, D. Khaghani, *et al.*, Time-resolved x-ray imaging of the current filamentation instability in solid-density plasmas, *Nature Communications* (2026).

[67] M. Cerchez, M. Swantusch, M. Toncian, X. M. Zhu, R. Prasad, T. Toncian, C. Rödel, O. Jäckel, G. G. Paulus, A. A. Andreev, and O. Willi, Enhanced energy absorption of high intensity laser pulses by targets of modulated surface, *Applied Physics Letters* **112**, 221103 (2018).